Prev. Nutr. Food Sci. 2019;24(4):442-448
https://doi.org/10.3746/pnf.2019.24.4.442
pISSN 2287-1098 · eISSN 2287-8602

Anti-Photoaging Effect of Korean Mint (*Agastache rugosa* Kuntze) Extract on UVB-Irradiated Human Dermal Fibroblasts

Heewon Seo, Changhee Kim, Mi-Bo Kim, and Jae-Kwan Hwang

Department of Biotechnology, College of Life Science and Biotechnology, Yonsei University, Seoul 03722, Korea

ABSTRACT: Ultraviolet B (UVB) irradiation-induced photoaging leads to wrinkles, dryness, and skin roughness. UVB irradiation activates the production of reactive oxygen species (ROS) and stimulates the mitogen-activated protein kinase (MAPK)/activator protein-1 (AP-1) signaling pathway, which promotes expression of matrix metalloproteinases (MMPs) and inflammatory cytokines. The current study aimed to assess the anti-photoaging activity of *Agastache rugosa* extract (ARE) on UVB-treated human dermal fibroblasts. ARE treatment reduced the overproduction of ROS and promoted mRNA expression of anti-oxidant enzymes. ARE treatment significantly inactivated the MAPK/AP-1 signaling pathway, which downregulated the expression of MMPs. Moreover, ARE promoted the production of type-I procollagen and upregulated mRNA expression of collagen genes. Additionally, ARE suppressed the expression of inflammatory cytokines, including interleukin (IL)-1β, IL-6, and IL-8, by preventing expression of nuclear factor-kappa B. Collectively, our findings show that ARE could be a potential candidate for anti-photoaging treatment.

Keywords: *Agastache rugosa* Kuntze, anti-photoaging, collagen, Korean mint, matrix metalloproteinase

INTRODUCTION

Skin aging involves intrinsic and extrinsic aging (Ramos-e-Silva et al., 2013). Intrinsic aging occurs with the passage of time, whereas extrinsic aging occurs owing to exposure to external factors, such as harmful chemicals, air pollutants, and ultraviolet B (UVB) irradiation (Kohl et al., 2011). Extrinsic aging resulting from long-term exposure to UVB irradiation is called photoaging. During this process, UVB irradiation penetrates into the dermis and induces breakdown of skin components; this is associated with skin inflammation, DNA damage, and oxidative stress (Matsumura and Ananthaswamy, 2004). In particular, excessive generation of reactive oxygen species (ROS), a major element involved in stimulating oxidative stress, damages skin cells, which degrades and disorganizes extracellular matrix (ECM) components (Kim et al., 2015).

UVB irradiation-induced ROS production activates mitogen-activated protein kinases (MAPKs), subsequently stimulating to formation of the activator protein-1 (AP-1) (Rabe et al., 2006; Heng, 2013; Lu et al., 2016). AP-1 increases the expression of matrix metalloproteinases (MMPs), which stimulate breakdown of ECM components, especially collagens (Watson et al., 2014). Degrading collagens, main components involved in supporting dermal layers, lead to the destruction and collapse of skin structure (Quan et al., 2004; Chen et al., 2015). Therefore, downregulating MMP expression is an effective strategy to prevent and delay the development of photoaging-related symptoms, such as wrinkle formation and thickening in UVB-exposed skin (Bae et al., 2010). In terms of new collagen formation in the ECM, AP-1 complex blocks type-I procollagen production and downregulates collagen gene expression in UVB-exposed skin cells (Kammeyer and Luiten, 2015). Thus, photoaging is closely associated with both stimulating collagen breakdown and blocking collagen formation by suppressing type-I collagen synthesis and collagen gene expression (Sun et al., 2016). Additionally, exposure to UVB irradiation enhances translocation of nuclear factor kappa-B (NF-κB) to the nucleus where it is mainly involved transcription of inflammatory cytokines (Pillai et al., 2005). The inflammatory responses induced by activation of NF-κB in UVB-exposed skin cells lead to MMP overexpression and collagen degradation (Bai et al., 2015).

Agastache rugosa Kuntze, also known as Korean mint, is mainly found in Korea, Japan, and China. *A. rugosa* has

Received 26 July 2019; Accepted 18 September 2019; Published online 31 December 2019

Correspondence to Jae-Kwan Hwang, Tel: +82-2-2123-5881, E-mail: jkhwang@yonsei.ac.kr
Author information: Heewon Seo (Graduate Student), Changhee Kim (Graduate Student), Mi-Bo Kim (Researcher), Jae-Kwan Hwang (Professor)

been used as a food source and in traditional medicines to cure disease because it has varied bioactivities, which encompass anti-oxidant, anti-melanogenic, anti-atherogenic, anti-inflammatory, and anti-fungal properties (Hong et al., 2001; Lee et al., 2017). Previously, *A. rugosa* leaf extract was shown to reduce photoaging by activating glutathione and superoxide dismutase (SOD) in human keratinocytes (HaCaT) (Oh et al., 2016). However, the anti-photoaging effect of *A. rugosa* extract (ARE) and the underlying mechanisms in human dermal fibroblasts (HS68) have not yet been proven. Here, we determined the attenuating effect of ARE on photoaging in UVB-treated human dermal fibroblasts by examining the underlying molecular mechanisms.

MATERIALS AND METHODS

Preparation of ARE

ARE was obtained from Cosmax NBT (Seoul, Korea). The dried aerial parts of *A. rugosa* were extracted with water at 95°C for 4 h. ARE filtrates were evaporated, and the final yield of ARE was 10% (w/w).

Cell culture and UVB irradiation

HS68 cells were purchased from the American Type Culture Collection (Manassas, VA, USA). The cells were maintained in Dulbecco's modified Eagle's medium (HyClone Laboratories, Inc., Logan, UT, USA) containing 120 U/mL penicillin and 75 μg/mL streptomycin (Invitrogen, Grand Island, NY, USA), and 10% fetal bovine serum (HyClone Laboratories, Inc.) in a humidified atmosphere of 5% CO_2 at 37°C. To induce photoaging, the cells were exposed to UVB irradiation (15 mJ/cm^2) by using a UV crosslinker CL-1000M (Ultra-Violet Products Ltd., Cambridge, UK).

Cell viability

After UVB irradiation, HS68 cells were treated with several concentrations of ARE dissolved in serum-free medium for 24 h. After 24 h, the cells were incubated with 3-(4,5-dimethylthiazol-2-yl)-2,5-diphenyltetrazolium bromide (MTT; Sigma-Aldrich Co., St. Louis, MO, USA) solution (0.5 mg/mL) for 4 h in 5% CO_2 atmosphere at 37°C. After the removal of MTT solution, the absorbance of insoluble formazan dissolved in dimethyl sulfoxide was recorded using a VERSAmax tunable microplate reader (Molecular Devices Inc., Sunnyvale, CA, USA) at 540 nm. No significant cytotoxicity of ARE (up to 20 μg/mL) was observed (data not shown). Therefore, ARE (≤20 μg/mL) was used for further experiments.

Measurement of ROS production

After treatment with ARE and UVB exposure, cells were incubated with 2,7-dichlorofluorescein diacetate (Sigma-Aldrich Co.) in a CO_2 incubator at 37°C for 30 min. Subsequently, the cellular fluorescence was recorded using a SpectraMax Gemini EM microplate spectrofluorometer (Molecular Devices Inc.).

Western blot analysis

Cells were lysed with NP40 lysis buffer (Elpis-Biotech, Daejeon, Korea) supplemented with 0.2% protease inhibitor cocktail (Sigma-Aldrich Co.). After centrifugation at 16,000 *g* at 4°C for 15 min, the concentration of protein in the supernatant was evaluated by Bradford solution (Bio-Rad Laboratories, Inc., Hercules, CA, USA) with bovine serum albumin (bioWORLD, Dublin, OH, USA) used as a standard. Equal amounts of proteins in each group were subjected to 8∼10% sodium dodecyl sulfate-polyacrylamide gel electrophoresis for 90 min at 110 V. The separated proteins were transferred onto nitrocellulose blotting membranes (GE Healthcare, Piscataway, NJ, USA) for 1 h at 110 V. After nonspecific sites were blocked with 5% skimmed milk (Difco Laboratories Inc., Detroit, MI, USA), membranes were immunoblotted with primary antibodies against NF-κB, phospho (p)-p38, p-extracellular signal-regulated kinase (p-ERK), p-c-Jun N-terminal kinases (p-JNK), and c-Fos (Santa Cruz Biotechnology Inc., Santa Cruz, CA, USA.); and p-c-Jun, c-Jun, ERK, JNK, p38, and α-tubulin (Cell Signaling Technology, Danvers, MA, USA) at room temperature for 4 h. After washing three times in Tris-buffered saline (Dynebio, Gyeonggi, Korea) containing Tween 20, membranes were incubated with horseradish peroxidase-conjugated goat anti-rabbit or anti-mouse secondary antibodies (Bethyl Laboratories, Montgomery, TX, USA) at room temperature for 1 h. Enhanced chemiluminescence solution (Amersham BioSciences UK Ltd., Little Chalfont, UK) was used to develop the membranes. The band of protein was visualized using a G:BOX EF imaging system (Syngene, Cambridge, UK) and the GeneSys program.

Measurement of type-I procollagen contents

After treatment with ARE and UVB exposure, the type-I procollagen content of the medium was evaluated using a human procollagen I alpha 1 enzyme-linked immunosorbent assay kit (Abcam, Cambridge, MA, USA), according to the company's protocol. Absorbance was recorded using a VERSAmax tunable microplate reader (Molecular Devices Inc.) at 450 nm.

Reverse transcription-polymerase chain reaction (RT-PCR)

RNAiso Plus (Takara Bio Inc., Kusatsu, Japan) was used for isolation of total RNA from cells. The quantity and quality of the isolated mRNA were spectrophotometrically determined using a NanoDrop Lite spectrophotometer (Thermo Fisher Scientific Inc., Waltham, MA, USA). The

mRNA was reverse-transcribed to cDNA with RT PreMix (Elpis Biotech, Daejeon, Korea). Next, the cDNA of target genes was amplified using specific primers and HiPi PCR PreMix (Elpis Biotech). The list of primer sequences is shown in Table 1. Amplification was carried out over 25～30 cycles; denaturation for 30 s at 94°C, annealing for 1 min at 56～60°C, and extension for 1 min at 72°C. PCR experiments were carried out using a SimpliAmp Thermal Cycler (Applied Biosystems, Hercules, CA, USA). The amplified cDNA was stained with Loading star (Dynebio) and separated for 30 min in a Mupid electrophoresis chamber (Advance, Tokyo, Japan) on 1.5% agarose gel. The bands of target genes were visualized with G:BOX EF imaging system (Syngene) and GeneSys program.

Statistical analysis

All experiments were carried out three or more times. Data are shown as the mean±standard deviation (SD) and were analyzed using one-way analysis of variance (ANOVA). Intergroup differences were evaluated by Scheffe's test using SPSS 24.0 (SPSS Inc., Chicago, IL, USA). Statistical significance is indicated by $P<0.05$ or $P<0.01$. Hash tags and astericks denote significant differences compared to control cells and UVB-treated cells, respectively.

Table 1. Nucleotide sequences of primers using in reverse transcription-polymerase chain reaction (RT-PCR) experiments

Gene		Sequence (5′→3′)
Catalase	Forward	GCCACAGGAAAGTACCCCTC
	Reverse	CGGTGAGTGTCAGCATAGGC
SOD	Forward	ATGGCGACGAAGGCCGTGTG
	Reverse	GACCACCAGTGTGCGGCCAA
GPx	Forward	TGGGCATCAGGAGAACGCCA
	Reverse	TGCGTAGGGGCACACCGTCA
COL1A1	Forward	CACGACAAAGCAGAAACATC
	Reverse	ACACATCAAGACAAGAACGAG
COL3A1	Forward	TGGTGCCCCTGGTCCTTGCT
	Reverse	TACGGGGCAAAACCGCCAGC
COL4A1	Forward	TCCTGGCCTCCAGGGAATTA
	Reverse	ATCAACAGATGGGGTGCCTG
COL7A1	Forward	CTGGGAGAGAAGGTCGTGATGG
	Reverse	TCCACATTCGGCACACTTCC
MMP-1	Forward	AAGTCAAGTTTGTGGCTTATGG
	Reverse	GACTCATGTCTCCTGTCTCTTTCT
MMP-2	Forward	CATACAAAGGGATTGCCAGGAC
	Reverse	ATCGCTCCAGACTTGGAAGG
MMP-9	Forward	TCTATGGTCCTCGCCCTGAA
	Reverse	CATCGTCCACCGGACTCAAA
MMP-13	Forward	CTATGGTCCAGGAGATGA AG
	Reverse	AGAGTCTTGCCTGTATCCTC
IL-1β	Forward	AGCCATGGCAGAAGTACCTG
	Reverse	TCCATGGCCACAACAACTGA
IL-6	Forward	ATGAGGAGACTTGCCTGGTG
	Reverse	ACAACAATCTGAGGTGCCCA
IL-8	Forward	CCAGGAAGAAACCACCGGAA
	Reverse	CCTCTGCACCCAGTTTTCCT
GAPDH	Forward	CTCCTGTTCGACAGTCAGCC
	Reverse	TCGCCCCACTTGATTTTGGA

SOD, superoxide dismutase; GPx, glutathione peroxidase; COL1A1, collagen type I alpha 1; COL3A1, collagen type III alpha 1; COL4A1, collagen type IV alpha 1; COL7A1, collagen type VII alpha 1; MMP, matrix metalloproteinase; IL, interleukin; GAPDH, glyceraldehyde-3-phosphate dehydrogenase.

RESULTS AND DISCUSSION

ARE suppresses ROS production and increases anti-oxidant enzyme expression.

Excessive production of ROS is a major cause of photoaging in UVB-irradiated skin, and can further induce oxidative stress and MMP expression (Park et al., 2014). Thus, inhibition of UVB-induced ROS production could be an effective strategy to prevent photoaging. The ability of ARE to scavenge free radicals, and thereby exert anti-oxidant effects, was previously reported (Desta et al., 2016). Moreover, the phytochemicals, acacetin, and rosmarinic acid, which are present in ARE, have been reported to possess anti-oxidant activities (Chen et al., 1990; Kim et al., 1999). Based on these studies, we evaluated the anti-oxidant properties of ARE in UVB-exposed human dermal fibroblasts by examining total levels of intracellular ROS. UVB irradiation markedly increased ROS generation; however, ARE treatment dose-dependently alleviated ROS production by 92% (10 μg/mL) and 142% (20 μg/mL), compared with UVB-treated HS68 cells (Fig. 1A). These results indicate that ARE exhibits anti-oxidant activity by suppressing UVB-induced ROS production. We also examined mRNA expression of anti-oxidant enzymes in UVB-treated HS68 cells. It was reported that UVB-induced ROS led to cellular senescence in dermal fibroblasts (Yang and Li, 2015). As anti-oxidant enzymes protect skin from UVB-induced thickening and wrinkle formation, it may be necessary to enhance the activities of these enzymes to prevent photoaging (Draelos, 2007). According to a previous study, linarin, an active compound in ARE, markedly increased expression of the major anti-oxidant enzyme catalase in lipopolysaccharide-stimulated mouse lung tissues (Han et al., 2018). We evaluated mRNA expression of the anti-oxidant enzymes catalase, SOD, and glutathione peroxidase (GPx) in cells treated with ARE. UVB irradiation reduced expression of all three transcripts; however, mRNA expression levels of these enzymes were markedly elevated after ARE treatment (Fig. 1B). Taken together, the reduction of UVB-stimulated ROS production and elevated expression of anti-oxidant enzymes suggest that ARE has potent anti-oxidant properties.

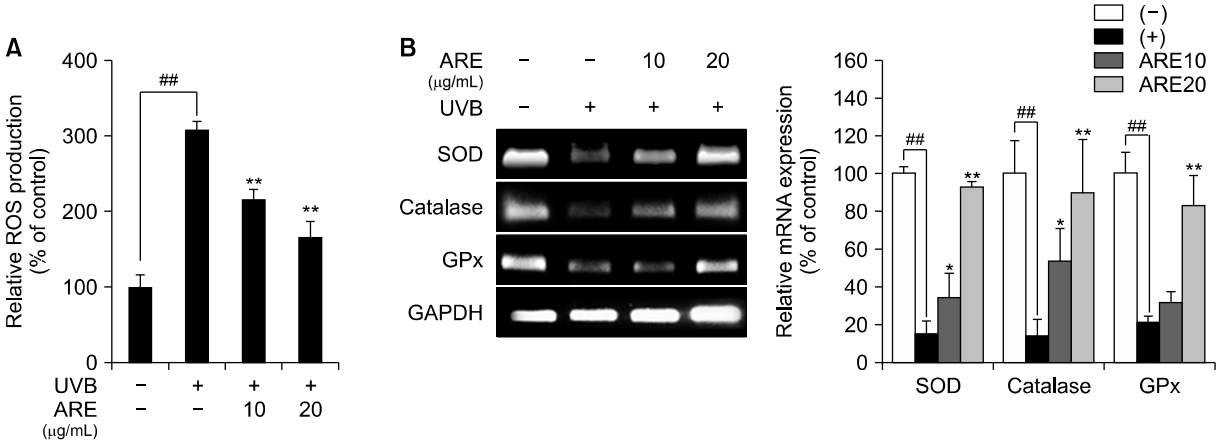

Fig. 1. Anti-oxidant effect of *Agastache rugosa* extract (ARE). (A) Effect of ARE on reactive oxygen species (ROS) production in Ultraviolet B (UVB)-treated HS68 cells. (B) Reverse transcription-polymerase chain reaction analysis of the expression of catalase, superoxide dismutase (SOD), and glutathione peroxidase (GPx) after ARE (10 and 20 μg/mL) treatment. Glyceraldehyde-3-phosphate dehydrogenase (GAPDH) was used as a housekeeping gene. Data are expressed as mean±SD of three independent experiments. $^{\#\#}P<0.01$ compared with the control group. $^{*}P<0.05$ and $^{**}P<0.01$ compared with the UVB-treated cells.

ARE suppresses UVB-induced MMP expression through the downregulation of the MAPK/AP-1 pathway.

UVB irradiation stimulates MAPKs, which promotes heterodimerization of proteins in the AP-1 complex. Enhancement of the MAPK/AP-1 signaling pathway promotes upregulation of MMP expression, which subsequently results in breakdown of ECM components, such as elastic fibers, glycosaminoglycans, and collagens. Consequently, this signaling cascade results in photoaging-related phenotypes, including wrinkle formation, epidermal thickening, and skin dryness (Chiang et al., 2012). It was reported that UVB exposure upregulated the pro-MMP-2 and -9 expression; however, probiotic-fermented ARE decreased the MMP expression in UVB-induced HaCaT cells (Shin et al., 2018). Based on this effect of ARE, we evaluated the expression of MMPs, MAPK, and AP-1 in UVB-irradiated HS68 cells. UVB treatment markedly increased MMP mRNA expression; however, treatment with ARE significantly decreased their expression (Fig. 2A). In this study, the MAPK signaling pathway was activated in the UVB-exposed cells. However, ARE significantly decreased MAPK expression, compared with UVB-irradiated HS68 cells (Fig. 2B). In comparison with untreated cells, UVB irradiation significantly upregulated protein expression of the AP-1 components p-c-Jun and c-Fos, whereas ARE downregulated p-c-Jun and c-Fos (Fig. 2C). Collectively, these data indicate that ARE decreases UVB-induced MMPs expression by inactivating the MAPK/AP-1 signaling pathway.

ARE increases type-I procollagen production and collagen expression.

UVB irradiation stimulates collagen breakdown by increasing the expression of MMPs and downregulates expression of collagen genes by activating the AP-1 complex (Chen et al., 2015). These responses alter the ECM architecture, resulting in wrinkle formation, elastosis, and skin dryness (Kammeyer and Luiten, 2015). Since ARE was revealed to reduce MMP expression by inhibiting MAPK/AP-1 cell signaling in UVB-treated HS68 cells, we evaluated the effect of ARE on regulation of genes related to collagen synthesis and production of type-I procollagen. The expression of the collagen genes [collagen type I α 1 (COL1A1), collagen type III α 1 (COL3A1), collagen type IV α 1 (COL4A1), and collagen type VII α 1 (COL7A1)] was significantly reduced in UVB-treated HS68 cells. However, ARE markedly upregulated mRNA expression of collagen genes (Fig. 3A). ARE treatment prevented UVB irradiation from reducing type-I procollagen production in a dose-dependent manner. Specifically, at a dose of 20 μg/mL, ARE increased type-I procollagen content by 27% (Fig. 3B). Consistent with these current results, *A. rugosa* recovered skin barrier function by increasing expression of collagens in atopic dermatitis-induced mice (Seo, 2014). This study demonstrates that ARE attenuates skin photoaging by activating type-I procollagen production and improving collagen synthesis in UVB-irradiated HS68 cells.

ARE inhibits UVB-induced inflammation.

Previous study showed that UVB irradiation elevated inflammatory responses by activating NF-κB and stimulating expression of NF-κB-mediated inflammatory cytokines (Bradley, 2008). UVB-induced inflammatory responses upregulate MMP expression, resulting in skin dehydration, psoriasis, and erythema (Schnegg et al., 2012). Here, mRNA expression of inflammatory mediators was examined in UVB-exposed HS68 cells. UVB irradiation elevated protein expression of NF-κB, which was inhibited by ARE (Fig. 4A). In addition, mRNA expression of NF-κB-stimulated inflammatory cytokines was decreased in calls treated with ARE, compared with

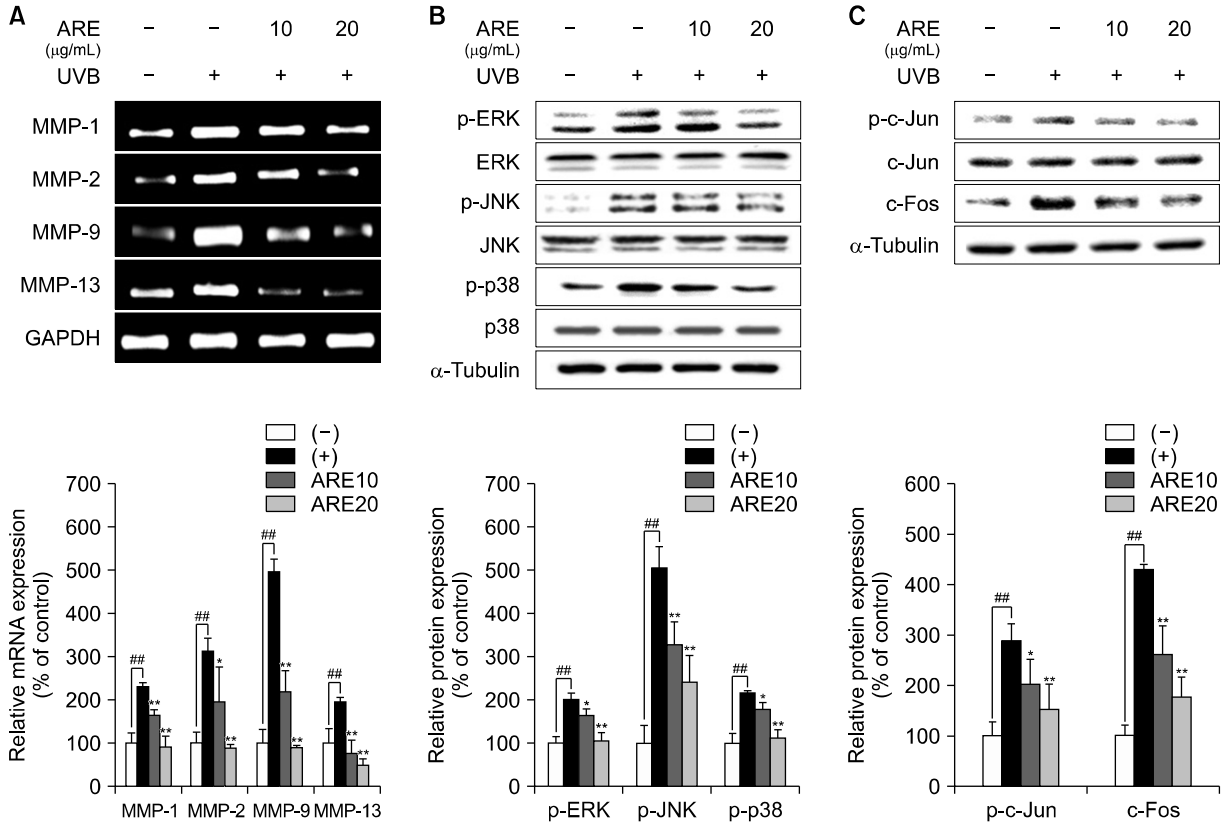

Fig. 2. Effect of *Agastache rugosa* extract (ARE) on ultraviolet B (UVB)-induced matrix metalloproteinase (MMP) expression and mitogen-activated protein kinase (MAPK)/activator protein-1 (AP-1) signaling. (A) Reverse transcription-polymerase chain reaction analysis of the expression of matrix metalloproteinase (MMP)-1, MMP-2, MMP-9, and MMP-13 after ARE (10 and 20 μg/mL) treatment. (B) Western blot analysis of the expression of p-extracellular signal-regulated kinase (ERK), ERK, p-c-Jun N-terminal kinase (JNK), JNK, p-p38, and p38 after ARE (10 and 20 μg/mL) treatment. (C) Western blot analysis of the expression of p-c-Jun, c-Jun, and c-Fos after ARE (10 and 20 μg/mL) treatment. α-Tubulin and glyceraldehyde-3-phosphate dehydrogenase (GAPDH) were used as housekeeping genes. Data are expressed as mean±SD of three independent experiments. $^{\#\#}P<0.01$ compared with the control group. $^{*}P<0.05$ and $^{**}P<0.01$ compared with the UVB-treated cells.

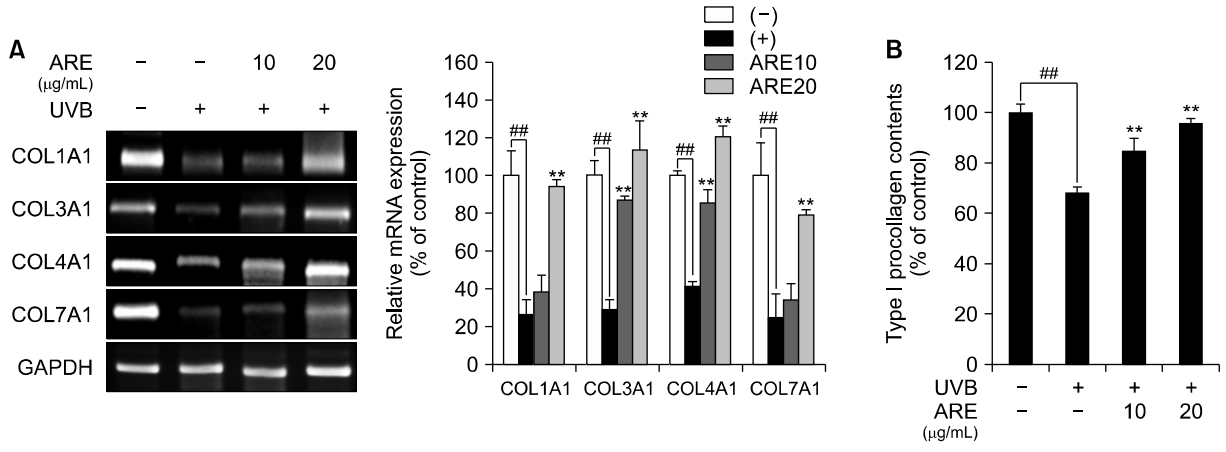

Fig. 3. Effect of *Agastache rugosa* extract (ARE) on collagen synthesis and type-I procollagen production. (A) Reverse transcription-polymerase chain reaction analysis of the expression of collagen type I alpha 1 (COL1A1), collagen type III alpha 1 (COL3A1), collagen type IV alpha 1 (COL4A1), and collagen type VII alpha 1 (COL7A1) after ARE (10 and 20 μg/mL) treatment. (B) Type-I procollagen content after ARE (10 and 20 μg/mL) treatment. Glyceraldehyde-3-phosphate dehydrogenase (GAPDH) was used as a housekeeping gene. Data are expressed as mean±SD of three independent experiments. $^{\#\#}P<0.01$ compared with the control group. $^{**}P<0.01$ compared with the UVB-treated cells.

UVB-irradiated HS68 cells (Fig. 4B). The anti-inflammatory effect of ARE was reported in an osteosarcoma cell line, accompanied by downregulation of interleukin-1β and tumor necrosis factor-α (Oh et al., 2005). Consistent with this report, our data showed that ARE exhibited strong anti-inflammatory effects, thereby playing a critical

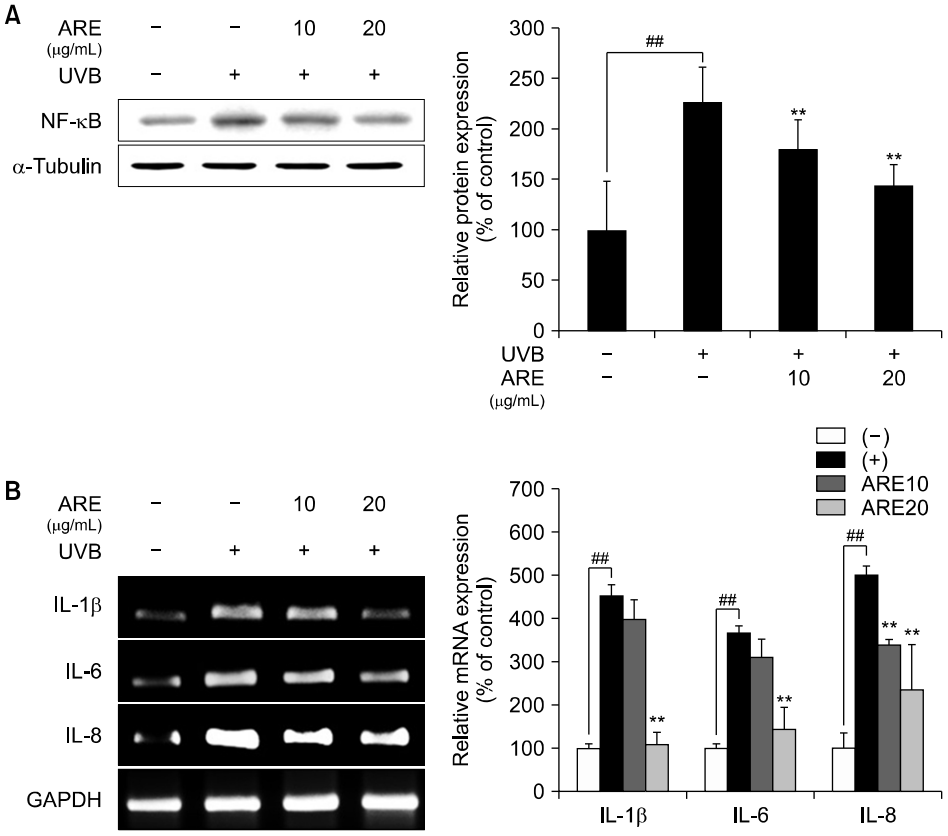

Fig. 4. Effect of *Agastache rugosa* extract (ARE) on inflammatory cytokine levels. (A) Western blot analysis of the expression of nuclear factor-kappa B (NF-κB) after ARE (10 and 20 μg/mL) treatment. (B) Reverse transcription-polymerase chain reaction analysis of the expression of IL-1β, IL-6, and IL-8 after ARE (10 and 20 μg/mL) treatment. α-Tubulin and GAPDH were used as housekeeping genes. Data are expressed as mean±SD of three independent experiments. $^{\#\#}P<0.01$ compared with the control group, $^{**}P<0.01$ compared with the UVB-treated cells.

role in anti-photoaging property by suppressing expression of NF-κB and pro-inflammatory cytokines. Taken together, these results suggest that ARE could be used as an anti-photoaging agent owing to its alleviation of UVB-induced skin inflammatory responses.

In this study, the anti-photoaging effect of ARE was investigated in UVB-irradiated human dermal fibroblasts. ARE suppressed UVB-induced oxidative stress by reducing production of ROS and by increasing expression of anti-oxidant enzymes. In addition, ARE attenuated UVB-activated MAPK/AP-1 signaling, resulting in downregulation of MMP expression. Moreover, ARE both upregulated expression of collagen genes and increased production of procollagen. Further, ARE alleviated UVB-stimulated inflammatory responses by suppressing expression of inflammatory cytokines. Collectively, our findings suggest that ARE could be a potential candidate for skin anti-photoaging treatment. To develop ARE as a novel anti-photoaging agent, potentially as an ingredient in functional foods or nutraceuticals, the anti-photoaging effect of ARE should be verified in animal studies and clinical trials.

ACKNOWLEDGEMENTS

This work was supported by the World Class 300 Project R&D Program (S2435140) funded by the Small and Medium Business Administration (SMBA, Republic of Korea).

AUTHOR DISCLOSURE STATEMENT

The authors declare no conflict of interest.

REFERENCES

Bae JY, Choi JS, Kang SW, Lee YJ, Park J, Kang YH. Dietary compound ellagic acid alleviates skin wrinkle and inflammation induced by UV-B irradiation. Exp Dermatol. 2010. 19:e182-e190.

Bai B, Liu Y, You Y, Li Y, Ma L. Intraperitoneally administered biliverdin protects against UVB-induced skin photo-damage in hairless mice. J Photochem Photobiol B. 2015. 144:35-41.

Bradley JR. TNF-mediated inflammatory disease. J Pathol. 2008. 214:149-160.

Chen B, Li R, Yan N, Chen G, Qian W, Jiang HL, et al. Astragaloside IV controls collagen reduction in photoaging skin by improving transforming growth factor-β/Smad signaling suppression and inhibiting matrix metalloproteinase-1. Mol Med Rep. 2015. 11:3344-3348.

Chen YT, Zheng RL, Jia ZJ, Ju Y. Flavonoids as superoxide scavengers and antioxidants. Free Radic Biol Med. 1990. 9:19-21.

Chiang HM, Chen HC, Lin TJ, Shih IC, Wen KC. *Michelia alba* extract attenuates UVB-induced expression of matrix metalloproteinases via MAP kinase pathway in human dermal fibroblasts. Food Chem Toxicol. 2012. 50:4260-4269.

Desta KT, Kim GS, Kim YH, Lee WS, Lee SJ, Jin JS, et al. The polyphenolic profiles and antioxidant effects of *Agastache rugosa* Kuntze (Banga) flower, leaf, stem and root. Biomed Chromatogr.

2016. 30:225-231.
Draelos ZD. The latest cosmeceutical approaches for anti-aging. J Cosmet Dermatol. 2007. 6:2-6.
Han X, Wu YC, Meng M, Sun QS, Gao SM, Sun H. Linarin prevents LPS-induced acute lung injury by suppressing oxidative stress and inflammation via inhibition of TXNIP/NLRP3 and NF-κB pathways. Int J Mol Med. 2018. 42:1460-1472.
Heng MC. Signaling pathways targeted by curcumin in acute and chronic injury: burns and photo-damaged skin. Int J Dermatol. 2013. 52:531-543.
Hong JJ, Choi JH, Oh SR, Lee HK, Park JH, Lee KY, et al. Inhibition of cytokine-induced vascular cell adhesion molecule-1 expression; possible mechanism for anti-atherogenic effect of *Agastache rugosa*. FEBS Lett. 2001. 495:142-147.
Kammeyer A, Luiten RM. Oxidation events and skin aging. Ageing Res Rev. 2015. 21:16-29.
Kim JB, Kim JB, Cho KJ, Hwang YS, Park RD. Isolation, identification, and activity of rosmarinic acid, a potent antioxidant extracted from Korean *Agastache rugosa*. J Korean Soc Agric Chem Biotechnol. 1999. 42:262-266.
Kim M, Park YG, Lee HJ, Lim SJ, Nho CW. Youngiasides A and C isolated from *Youngia denticulatum* inhibit UVB-induced MMP expression and promote type I procollagen production via repression of MAPK/AP-1/NF-κB and activation of AMPK/Nrf2 in HaCaT cells and human dermal fibroblasts. J Agric Food Chem. 2015. 63:5428-5438.
Kohl E, Steinbauer J, Landthaler M, Szeimies RM. Skin ageing. J Eur Acad Dermatol Venereol. 2011. 25:873-884.
Lee JJ, Lee JH, Gu MJ, Han JH, Cho WK, Ma JY. *Agastache rugosa* Kuntze extract, containing the active component rosmarinic acid, prevents atherosclerosis through up-regulation of the cyclin-dependent kinase inhibitors $p21^{WAF1/CIP1}$ and $p27^{KIP1}$. J Funct Foods. 2017. 30:30-38.
Lu J, Guo JH, Tu XL, Zhang C, Zhao M, Zhang QW, et al. Tiron inhibits UVB-induced AP-1 binding sites transcriptional activation on MMP-1 and MMP-3 promoters by MAPK signaling pathway in human dermal fibroblasts. PLoS One. 2016. 11: e0159998.
Matsumura Y, Ananthaswamy HN. Toxic effects of ultraviolet radiation on the skin. Toxicol Appl Pharmacol. 2004. 195:298-308.
Oh HM, Kang YJ, Kim SH, Lee YS, Park MK, Heo JM, et al. *Agastache rugosa* leaf extract inhibits the iNOS expression in ROS 17/2.8 cells activated with TNF-α and IL-1β. Arch Pharm Res. 2005. 28:305-310.
Oh Y, Lim HW, Huang YH, Kwon HS, Jin CD, Kim K, et al. Attenuating properties of *Agastache rugosa* leaf extract against ultraviolet-B-induced photoaging via up-regulating glutathione and superoxide dismutase in a human keratinocyte cell line. J Photochem Photobiol B. 2016. 163:170-176.
Park JE, Pyun HB, Woo SW, Jeong JH, Hwang JK. The protective effect of *Kaempferia parviflora* extract on UVB-induced skin photoaging in hairless mice. Photodermatol Photoimmunol Photomed. 2014. 30:237-245.
Pillai S, Oresajo C, Hayward J. Ultraviolet radiation and skin aging: roles of reactive oxygen species, inflammation and protease activation, and strategies for prevention of inflammation-induced matrix degradation—a review. Int J Cosmet Sci. 2005. 27:17-34.
Quan T, He T, Kang S, Voorhees JJ, Fisher GJ. Solar ultraviolet irradiation reduces collagen in photoaged human skin by blocking transforming growth factor-beta type II receptor/Smad signaling. Am J Pathol. 2004. 165:741-751.
Rabe JH, Mamelak AJ, McElgunn PJ, Morison WL, Sauder DN. Photoaging: mechanisms and repair. J Am Acad Dermatol. 2006. 55:1-19.
Ramos-e-Silva M, Celem LR, Ramos-e-Silva S, Fucci-da-Costa AP. Anti-aging cosmetics: facts and controversies. Clin Dermatol. 2013. 31:750-758.
Schnegg CI, Kooshki M, Hsu FC, Sui G, Robbins ME. PPARδ prevents radiation-induced proinflammatory responses in microglia via transrepression of NF-κB and inhibition of the PKCα/MEK1/2/ERK1/2/AP-1 pathway. Free Radic Biol Med. 2012. 52:1734-1743.
Seo YM. Recovery effect of blending oil on skin barrier damaged by atopic dermatitis. J East-West Nurs Res. 20:57-62.
Shin D, Lee Y, Huang YH, Lim HW, Jang K, Kim DD, et al. Probiotic fermentation augments the skin anti-photoaging properties of *Agastache rugosa* through up-regulating antioxidant components in UV-B-irradiated HaCaT keratinocytes. BMC Complement Altern Med. 2018. 18:196.
Sun Z, Park SY, Hwang E, Park B, Seo SA, Cho JG, et al. Dietary *Foeniculum vulgare* Mill extract attenuated UVB irradiation-induced skin photoaging by activating of Nrf2 and inhibiting MAPK pathways. Phytomedicine. 2016. 23:1273-1284.
Watson RE, Gibbs NK, Griffiths CE, Sherratt MJ. Damage to skin extracellular matrix induced by UV exposure. Antioxid Redox Signal. 2014. 21:1063-1077.
Yang Y, Li S. Dandelion extracts protect human skin fibroblasts from UVB damage and cellular senescence. Oxid Med Cell Longev. 2015. 2015:619560.